

# ADVANCED POOL BOILING HEAT SINKS MANUFACTURED BY SELECTIVE LASER MELTING AND EFFECT OF HEAT TREATMENT

Tianqing Wu<sup>1</sup>, Poh Seng Lee<sup>1,\*</sup>, John Mathew<sup>1</sup>, Chen-Nan Sun<sup>2</sup>, Beng Loon Aw<sup>2</sup>

1 Department of Mechanical Engineering, National University of Singapore, 9 Engineering Drive 1, Singapore 117575

2 Singapore Institute of Manufacturing Technology, 73 Nanyang Drive, Singapore 637662

\*Corresponding author. Tel.: +65-6516 4187

Email: pohseng@nus.edu.sg

## ABSTRACT

The rapid development of modern electronic devices urges an increasing need for better heat transfer techniques. Pool boiling heat transfer has great potential as it can provide high heat transfer capacity during the phase change of the working fluid. With the help of additive manufacturing technology, complex designs of pool boiling heat sinks can be achieved with selective laser melting (SLM) and they have shown great performances. In this study, heat sinks with one-layer and two-layer porous fin arrays are manufactured by SLM method using AlSi12 alloy powders and heat treated at 450°C in nitrogen. Their pool boiling performances have shown great enhancement compared with plain copper heat sinks and the heat treated heat sinks have shown the best result both in heat transfer coefficient (HTC) and critical heat flux (CHF). The visualization data is collected during the experiments and used to analyze the heat transfer mechanism.

**Keywords:** Pool boiling, two-phase heat transfer, porous structure, Selective Laser Melting

|   |   |
|---|---|
| 2 | top thermocouple in the conducting block    |
| 3 | middle thermocouple in the conducting block |
| 4 | bottom thermocouple in the conducting block |
| 5 | thermocouple immersed in the pool           |

## 1. Introduction

There is an increasing demand for more effective heat transfer techniques to satisfy the cooling needs of modern electronic devices like the high performance CPUs and GPUs. Pool boiling is a promising method because it can utilize the latent heat during the phase change of the working fluid. Many researchers have been working to push the limit of cooling performance of pool boiling heat transfer. However, due to the constraint of manufacturing techniques, the structures investigated are limited. Even though porous structures are favorable for pool boiling applications as demonstrated in [1], their product quality is hard to control and there may exist high thermal resistance between the sintered particles.

Additive manufacturing is a promising new technique that can broaden the design strategies for pool boiling heat sinks. By using the laser power, the metal powders can be melted and constructed in the exact same order as designed in the CAD software. Additive manufactured parts with micro-structures have been demonstrated in [2]. The pool boiling heat sinks are tested in FC-72 and the results showed more than 70% enhancement in both HTC and CHF compared to plain surface. For more complex porous structures, Wong and Leong [3] applied Selective Laser Melting (SLM) technique and manufactured heat sinks with different porous cell sizes and different layer numbers. The pool boiling experiments for these heat sinks were also conducted using FC-72 and they proved that the heat transfer performance was sensitive with the design parameters. Bigger structures manufactured by SLM can also be used to enhance the pool boiling performance. Hayes et al. [4] designed a hollow conical structure on top of normal heat sinks with plain and microchannel surfaces. The

## NONMENCLATURE

### Abbreviations

|            |  |
|------------|--|
| CHF        | critical heat flux, $W/cm^2$                         |
| HTC        | heat transfer coefficient, $kW/m^2K$                 |
| k          | thermal conductivity, $W/mK$                         |
| L          | length between thermocouple and heatsink surface, mm |
| ONB        | onset of nucleate boiling                            |
| $q''$      | heat flux, $W/cm^2$                                  |
| T          | temperature, °C                                      |
| x          | distance, mm   |
| $\Delta x$ | distance between two thermocouples, mm               |

### Subscripts

|     |  |
|-----|--|
| s   | heat sink surface                      |
| sat | saturated                              |
| 1   | thermocouple inserted in the heat sink |

heat sinks are manufactured using aluminum 6061 and the enhancement of heat transfer is credited to the separate liquid-vapor pathways generated by the structures. The previous research has demonstrated the application of additive manufacturing techniques in fabricating pool boiling heat sinks. However, the designs are still quite simple and the test pieces have not gone through any post processing. In this study, the porous fin arrays are directly printed on top of copper plain base using Aluminum Alloy powder (AlSi12) and the as-print and heat-treated heat sinks are compared for their pool boiling heat transfer performance. The pool boiling results are discussed with the high speed visualization images and the heat treatment of putting the heat sinks in nitrogen atmosphere for 6 hours at 450°C has been recognized as an effective method to further improve the heat transfer performance of additive manufactured heat sinks.

## 2. Experimental Methods

### 2.1 Test section

In order to illustrate the pool boiling heat transfer enhancement of SLM heat sinks, a plain copper piece is chosen as the benchmark as well as the printing base as shown in Fig.1. The effective heat transfer area is 10mm × 10mm and a Teflon tape is used to prevent heat loss from other areas. On the backside, a groove is cut outside the 10mm × 10mm area to ensure unidirectional heat transfer from the heat source to the top surface.

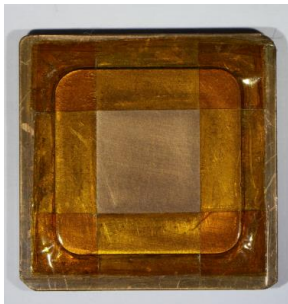


Fig.1. Image of plain copper test piece

Before testing with the heat sinks, the change in thermal properties of heat treated SLM products are investigated with slab samples. The image of slab samples can be found in Fig.2. The thickness of the samples is 1.93mm and the diameter is 55.8mm. These slab samples are printed using Concept Laser M2 cusing machine with the AlSi12 powder (3D Systems) and the measured density is higher than 99%. The thermal conductivity test of the samples is carried out in the Hot Disk TPS 2500s device using the ISO 22007-2.2 standard. The Kapton sensor 5501 is chosen for the test according

to the sample dimensions. During the measurement, two slab samples keep the sensor in between and insulation is applied on the other side of the sample. The Kapton sensor can both apply the heating energy to the slabs and measure the temperature drift. The measurements are carried out before and after heat treatment and the results are obtained as the average value of three repeated tests. The heat treatment is performed at 450°C for 6 hours under nitrogen atmosphere. The thermal conductivity of the slab samples before heat treatment is 104.0 W/mK while the result after the heat treatment is 190.2 W/mK, showing an enhancement of 82.8%. This enhancement of thermal conductivity is suggested to be the result of change of ultrafine eutectic microstructure that originally formed during the fast cooling process of SLM, as discussed in [5]. As thermal conductivity can play a significant role in heat transfer, this heat treatment process may affect the heat dissipation rate of pool boiling heat sinks. SLM heat sinks with one-layer and two-layer porous fin arrays are used as the samples for the test.



Fig.2. Image of slab samples used for thermal conductivity test

The image of heat sinks investigated for the effect of heat treatment process are shown in Fig.3. There is no significant change of the structure after the heat treatment. The detailed geometry of the one-layer design can be found in Fig.4. Before printing the structure, a 0.1mm layer is printed to ensure good connection between the fins and the copper base. For the one-layer porous fin structure, it has 10 fin arrays on the heat sink and there is a 0.3mm channel between every two arrays. Hexagon openings are designed on both top and side walls, leaving space for liquid and vapor to pass. The designs are made to generate separation of liquid and vapor pathways and to enhance the pool boiling heat transfer through macroconvection. Similar mechanisms are demonstrated in [6-7]. The two-layer structure shares the same dimension of fins and openings of the one-layer structure but the height of the whole structure is 1mm with two layers of openings on

the side instead of 0.5mm. All the SLM pieces are manufactured using an SLM machine. The printing power of 180W, printing layer thickness of 0.03mm, scan speed of 1176mm/s and hatch spacing of 0.085mm is used in the manufacturing process. Also, the Island scanning strategy is applied.

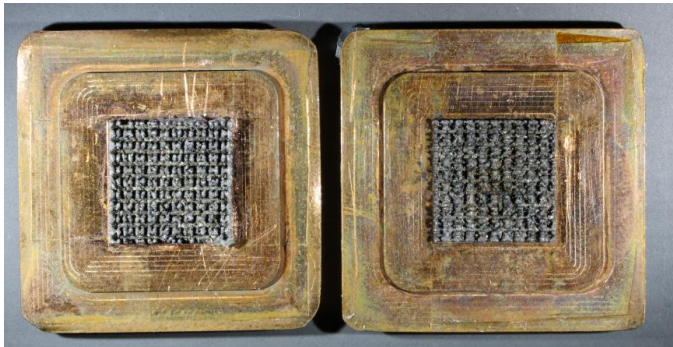


Fig.3. Image of heat sinks with porous channel arrays manufactured by SLM method. The heat sink shown on the left side is the two-layer structure while that on the right side is the one-layer structure

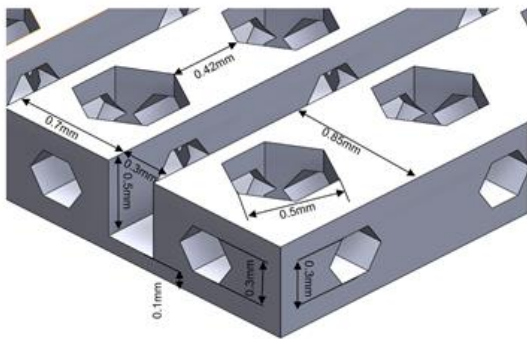


Fig.4. Geometry of the one-layer porous fin arrays design

## 2.2 Experimental Setup

The experimental setup used for the pool boiling tests of SLM heat sinks before and after heat treatment comprises of five main parts: the power supply system that supplies heating energy to the main ceramic heater (Watlow Ultramic® Advanced) and auxiliary water heater (Cartridge heater, Watlow®), the cooling system that runs deionized water through a copper coil and a liquid-air heat exchanger (Thermaxon, Model 735SPCOA01) to condense the vapor and redirect the liquid back to the experiment, the data acquisition system (NI cDAQ 9178) that consists of five T-type thermocouples (Omega) to measure and record the temperature data, a main test section where pool boiling takes place, and a visualization system that uses a high speed camera (FASTCAM SA5 1000K-M3) mounted on tripods near to the main test section.

Fig.5 shows the configuration of the main test section. The pool boiling chamber is made of Polycarbonate (PC) and an Acrylic window is designed on the side wall for visualization. The working fluid is deionized water and is sealed in the chamber by applying silicone sealant (Dow Corning® 734) between the chamber and copper heat sinks. The heat supplied to the ceramic heater is transferred from the bottom through a copper block to the heat sink surface. Thermal grease (Thermal Grizzly Kryonaut) is used to connect the copper block with the heat sinks. During the experiments, the heat sinks can be changed to different designs while all other parts remain the same. In the setup, one thermocouple is placed in the water to monitor the pool temperature and the auxiliary heater is used to maintain the water at saturation state. Other four thermocouples are inserted in the copper block to measure temperature data that can be used to calculate heat sink surface temperature and heat flux.

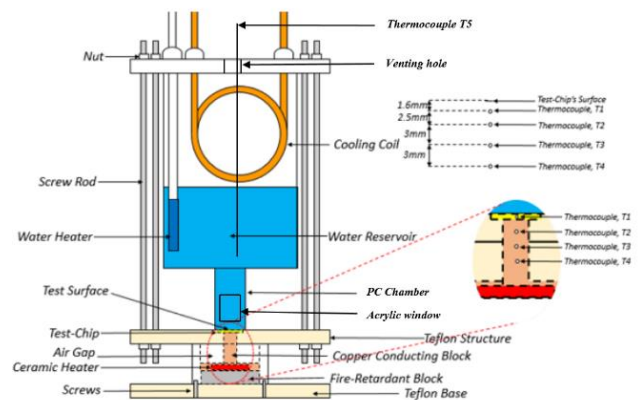


Fig. 5. Pool boiling experimental setup

## 2.3 Experimental Procedure and Data Reduction

Prior to all experiments, the thermocouples are calibrated using a calibrator (Fast-Cal Isotech). The deionized water in the pool boiling chamber would go through a two-hour degassing process to remove soluble gases before the heat flux is applied through the main ceramic heater. At the required heat flux, the temperature and visualization data is recorded when the steady state condition is reached for more than 5 minutes. After one condition is tested, the power supply is controlled to increase to a higher input point. These steps are repeated till the CHF is reached for the specific heat sink or the maximum temperature for the system is reached. The CHF condition can be determined when the temperature profile of the  $T_1$  suddenly increases for more than 10°C and the safe maximum temperature for the setup is taken as 400°C to prevent failure of the ceramic heater.

Using the experimental data of plain copper heat sink before heat treatment, the one dimensional heat transfer inside the copper block is confirmed following the method provided in [8]. In the experiments, the thermal conductivity ( $k$ ) of the copper is taken as a constant value,  $400\text{W/mK}$ . The total heat flux ( $q''$ ) dissipated through the heat sink surface is calculated as

$$q'' = -k \frac{dT}{dx} \quad (1)$$

$$\frac{dT}{dx} = \frac{T_4 - T_2}{\Delta x} \quad (2)$$

where  $\Delta x$  is 6mm. The surface temperature ( $T_s$ ) is taken as the temperature at the top of copper surface for all the heat sinks, it can be calculated as:

$$T_s = T_1 - q'' \left( \frac{L}{k} \right) \quad (3)$$

where  $L$  is 1.6mm. As the pool boiling setup is connected to the atmosphere, the saturation temperature of water is taken as  $100^\circ\text{C}$ . The HTC is calculated as the total heat flux divided by the wall super heat:

$$HTC = \frac{q''}{T_s - T_{sat}} \quad (4)$$

Using the methods proposed by Taylor [9], the uncertainty of the heat flux and HTC is estimated to be under  $\pm 5\%$  when the heat flux supplied is higher than  $40\text{W/cm}^2$ .

### 3. Experimental Results and Discussions

The boiling curves relating the projected heat flux and wall superheat of the copper surface are shown in Fig.6 to characterize the heat transfer performance of different heat sinks before and after heat treatment. The plain copper heat sink before heat treatment achieved a CHF of  $167.8\text{W/cm}^2$  at the wall superheat of  $17.1^\circ\text{C}$  and showed the highest HTC of  $98.0\text{kW/m}^2\text{K}$ . This result is close to the data of Bai et al. [1] and the variation may be due to different surface roughness and the size of the heating surface. After heat treatment, there is little change of the boiling curve for plain surface. This indicates that heat treatment has minimal influence on the pool boiling performance of CNC machined copper base.

For the SLM heat sinks before heat treatment, it can be seen that they show much improvement compared to plain surfaces. The one-layer structure surface reached CHF at  $312.2\text{W/cm}^2$  with the wall superheat of  $19.3^\circ\text{C}$ . The heat sink with two-layer structures reached a heat flux of  $453.2\text{W/cm}^2$  without the sign of CHF and the wall superheat is  $27.7^\circ\text{C}$ . These indicate the heat flux enhancement of 86% and 170%, respectively.

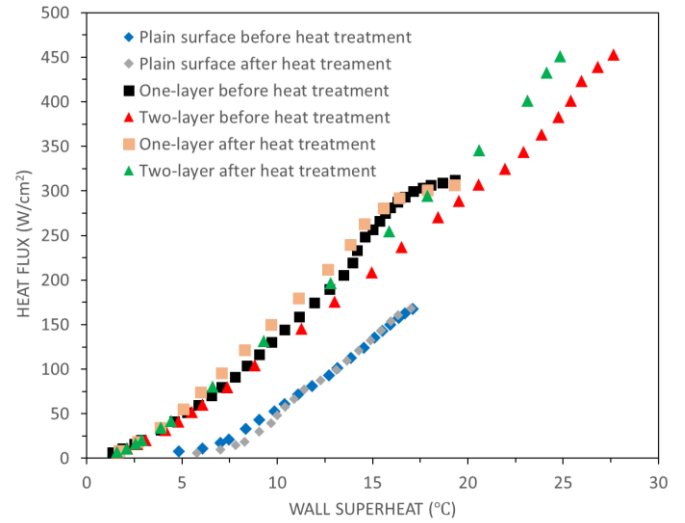


Fig.6. Nucleate boiling curves of heat sinks before and after heat treatment

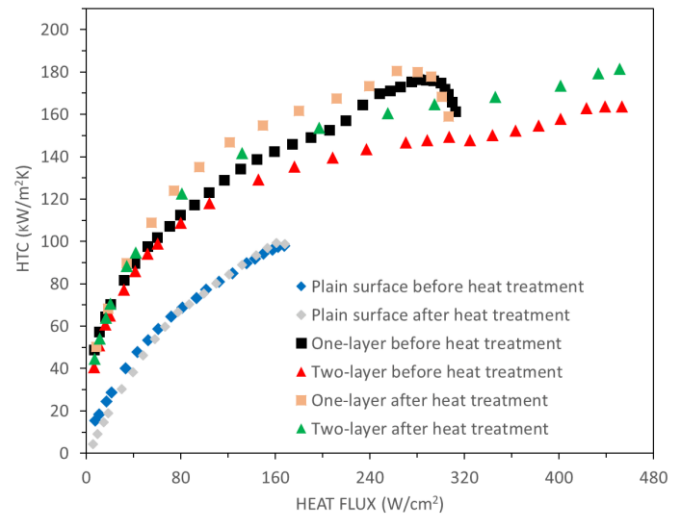


Fig.7. Heat transfer coefficient of different heat sinks before and after heat treatment versus the heat flux applied

The heat transfer performance plot is shown in Fig.7. The trend for plain and two-layer structures shows that HTC increases with heat flux. For the one-layer porous structure, however, the HTC first increases with heat flux and then the trend reverses at a turning point of about  $280\text{W/cm}^2$ . This can be explained by the periodic dry out situation over the heat sink surfaces when vapor generated blocks the liquid rewetting path to the surface. It is verified by the high temperature fluctuation in the recorded data. The highest HTC of  $176.5\text{kW/m}^2\text{K}$  and  $163.8\text{kW/m}^2\text{K}$  is obtained for one-layer and two layer porous structures, respectively. The SLM heat sinks before heat treatment can enhance the HTC of 80% and 67% compared to plain heat sink. The superior pool

boiling performance can be attributed to larger surface areas, more nucleation sites and enhanced macroconvection. The visualization image and proposed heat transfer mechanism for one-layer porous structure heat sinks before heat treatment, at heat flux of  $10.8\text{ W/cm}^2$ , are shown in Fig.8. During the boiling process, it is suggested that the liquid can be sucked in by the porous fins to the base area and the vapor are mostly removed from the channels. This separation of liquid and vapor pathways due to the porous fin array design enables the continuous supply of liquid from the pores to the nucleation sites in the fin base and corners. The resultant motion can result in much improvement in both HTC and CHF as demonstrated in [8].

As can be seen in Fig.6 and Fig.7, the heat treatment process does affect the boiling performance of SLM heat sinks. After treating in nitrogen at  $450^\circ\text{C}$  for 6 hours, the one-layer porous heat sink reached a CHF of  $306.8\text{ W/cm}^2$  with the wall superheat of  $19.3^\circ\text{C}$  and the two-layer structure reached a heat flux of  $451.2\text{ W/cm}^2$  at wall superheat of  $24.9^\circ\text{C}$  (no CHF). The highest HTC for the one-layer porous heat sink is  $180.5\text{ kW/m}^2\text{K}$  while for two-layer porous heat sink the value is  $181.5\text{ kW/m}^2\text{K}$ . Similar trend of heat transfer performance plot is observed for both heat sinks. The HTC increases with heat flux for the two-layer structure after heat treatment. A turning trend is observed for one-layer porous surface near the CHF area with the turning point of around  $260\text{ W/cm}^2$ , earlier than that of the heat sink before heat treatment. For the one-layer porous heat sink, the CHF value is very close before and after the heat treatment process (1.8 %) and the HTC is similar in both low heat flux and near CHF region. However, certain enhancement in pool boiling performance can be observed in medium heat flux region (around  $75\text{ W/cm}^2$  to  $170\text{ W/cm}^2$ ).

For the two-layer porous heat sinks, the HTC of heat treated test piece always has a better heat transfer performance and the difference increases with the heat flux. The biggest HTC difference is  $17.6\text{ kW/m}^2\text{K}$  at heat flux of about  $450\text{ W/cm}^2$ , showing the enhancement of 10.7%. At this heat flux, the two-layer porous structure shows no sign of dry-out. Images of pool boiling for the heat sinks with two-layer structures are shown in Fig.9. The images are taken from recorded high speed videos showing the same phase of pool boiling during the nucleation cycle. It can be seen from the images that there exists less space uncovered by the nucleating bubbles in the two-layer porous heat sink after the heat treatment suggesting that more vapor is generated.

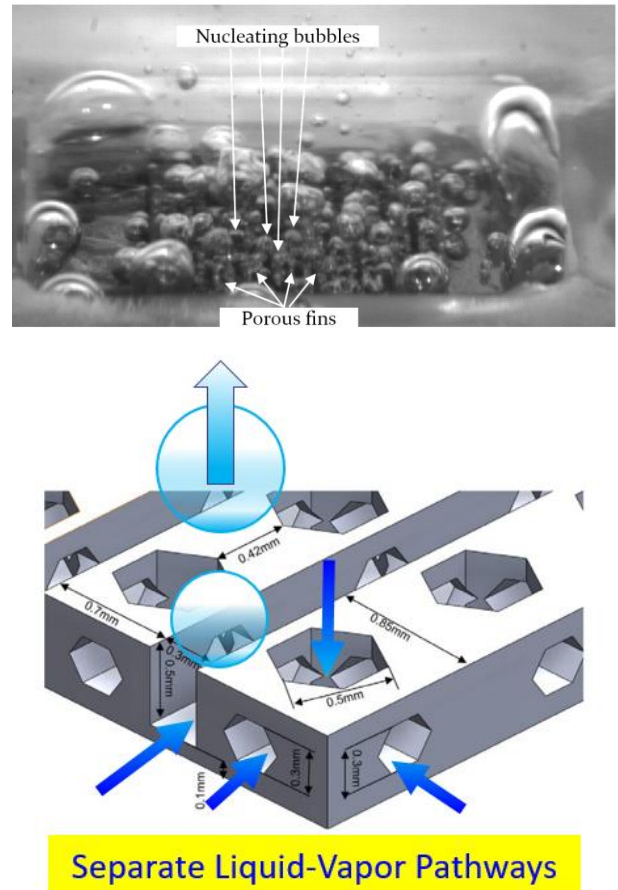


Fig.8. Photographic image and proposed heat transfer mechanisms for one-layer porous structure heat sinks before heat treatment at heat flux of  $10.8\text{ W/cm}^2$

The enhancement of pool boiling performance after the heat treatment is attributed to the increased thermal conductivity of AlSi12 after the heat treatment. With higher thermal conductivity, the temperature gradient of the SLM fin structure can be decreased and the average temperature along the structure surface is supposed to be closer to the base temperature. In the condition of heat flux of  $300\text{ W/cm}^2$ , the temperature difference at the top of the two-layer fin arrays before and after heat treatment can be as much as  $13.1^\circ\text{C}$  as calculated with the TPS 2500s hot disk measured value. At same heat flux, the heat treated heat sinks is suggested to have more activated nucleation sites in the porous structure and macroconvection is stronger because more vapor is generated to fuel the motion and the heat transfer between the sweeping liquid and the heating surface is improved. The influence of heat treatment is more significant with higher fin structures and higher heat fluxes except the near CHF region when bubble

generation is constrained by the liquid supply and more vapor generated may lead to the formation of liquid film and thus earlier CHF.

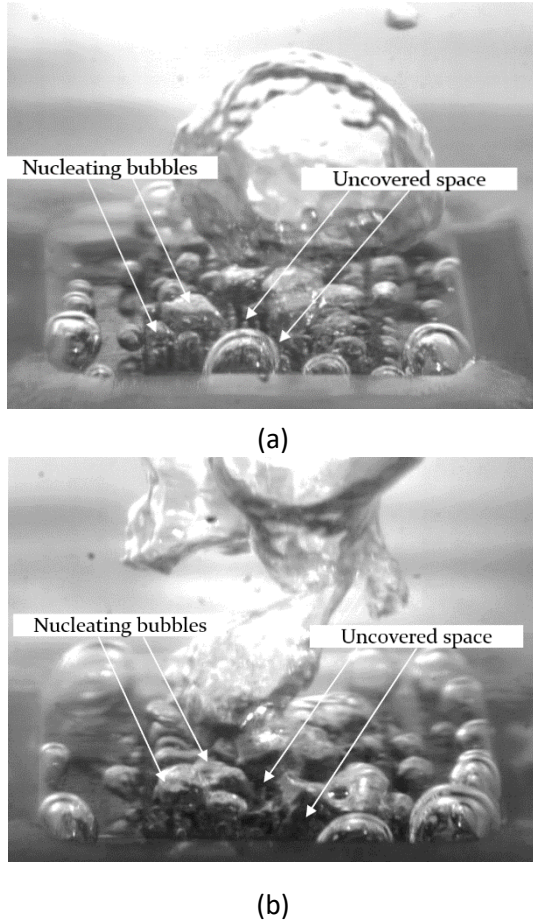


Fig.9. Images of pool boiling for (a) two-layer porous fin arrays before heat treatment at heat flux of  $41.4\text{W}/\text{cm}^2$ , (b) two-layer porous fin arrays after heat treatment at heat flux of  $41.8\text{W}/\text{cm}^2$

#### 4. Conclusions

Pool boiling experiments of SLM and plain heat sinks demonstrated that the heat treated test pieces have similar performance trend with the untreated ones and all the SLM pieces showed much enhancement compared to plain heat sinks.

It can also be concluded that the heat treatment does not show much influence on the CHF of one-layer porous fin structures. However, the heat treatment process can enhance the pool boiling performance in the medium heat flux region for the one-layer porous fin arrays and it can enhance the HTC of two-layer porous fin arrays in all heat fluxes. This enhancement can be attributed to the increased thermal conductivity of AISi12 structures after heat treatment and the influence is more significant with higher structures and higher heat flux. The presented study has demonstrated the possibility of using post

processing methods to further improve the performance of SLM pool boiling heat sinks and more treatment conditions or post processing methods can be investigated in the future.

#### Acknowledgments

Financial support for this study from Infocomm Media Development Authority (IMDA), Singapore (WBS No. R265-000-574-490) is gratefully acknowledged.

#### References

- [1] L. Bai, L. Zhang, G. Lin, and G. P. Peterson, "Pool boiling with high heat flux enabled by a porous artery structure," *Appl. Phys. Lett.*, vol. 108, no. 23, 2016.
- [2] J. Y. Ho, K. K. Wong, and K. C. Leong, "Saturated pool boiling of FC-72 from enhanced surfaces produced by Selective Laser Melting," *Int. J. Heat Mass Transf.*, vol. 99, pp. 107–121, 2016.
- [3] K. K. Wong and K. C. Leong, "Saturated pool boiling enhancement using porous lattice structures produced by Selective Laser Melting," *Int. J. Heat Mass Transf.*, vol. 121, pp. 46–63, 2018.
- [4] A. Hayes, P. A. Raghupathi, T. S. Emery, and S. G. Kandlikar, "Regulating flow of vapor to enhance pool boiling," *Appl. Therm. Eng.*, vol. 149, no. September 2018, pp. 1044–1051, 2019.
- [5] W. Li *et al.*, "Materials Science & Engineering A Effect of heat treatment on AISi10Mg alloy fabricated by selective laser melting: Microstructure evolution, mechanical properties and fracture mechanism," *Mater. Sci. Eng. A*, vol. 663, pp. 116–125, 2016.
- [6] S. G. Kandlikar, "Enhanced Macro-convection Mechanism with Separate Liquid-Vapor Pathways to Improve Pool Boiling Performance," *J. Heat Transfer*, vol. 139, no. May, pp. 1–11, 2016.
- [7] A. Jaikumar and S. G. Kandlikar, "Pool boiling enhancement through bubble induced convective liquid flow in feeder microchannels," *Appl. Phys. Lett.*, vol. 108, no. 4, 2016.
- [8] A. Jaikumar and S. G. Kandlikar, "Ultra-high pool boiling performance and effect of channel width with selectively coated open microchannels," *Int. J. Heat Mass Transf.*, vol. 95, pp. 795–805, 2016.
- [9] J. Taylor, *Introduction to Error Analysis, the Study of Uncertainties in Physical Measurements*, 2nd Edition. University Science Books, 1997.